AIAA JOURNAL
Vol. 36, No. 8, August 1998

Broadband Self-Noise from a Ducted Fan

Stewart A. L. Glegg* and Cyrille Jochault†
Florida Atlantic University, Boca Raton, Florida 33431

The prediction of broadband self-noise from ducted fans is described. The source mechanism is assumed to be the interaction of the turbulent boundary layer with the trailing edges of the fan blades. The source levels are obtained from the measurements of self-noise from isolated blades, and these measurements are corrected to give the in-duct sound power from a high-solidity fan. It has been found that the blade surface pressures are not uncorrelated on each fan blade, and corrections must be included for the scattering from multiple trailing edges. A method is introduced for coupling the modes in a circular duct to the modes of a linear cascade so that the sound power is not singular at the mode cut on frequencies. Results show that the in-duct sound power scales with the fifth power of the fan speed at low Mach numbers, but this changes to the sixth power or greater at high Mach numbers. The angle of attack of the blade increases the self-noise as 2.4 dB/deg, and there are significant increases in low-frequency noise when blade stall occurs.

Nomenclature

$A_{js}(\omega)$	= duct mode amplitude
$A_p(\gamma, \nu)$	= blade response function as in Eq. (26)
a	= duct radius
B	= number of blades on rotor
b	= blade span
c	= blade chord
d	= blade stagger
$F_n(r, \xi, \omega)$	= Fourier transform with respect to time of blade surface pressure on nth blade
$f_i(\boldsymbol{y}, \tau)$	= force per unit area applied to the fluid by the blade
$G(\boldsymbol{y}, \tau/\boldsymbol{x}, t)$	= Green's function
g	= function describing blade surface
g_n	= blade response function for rectilinear cascade
$H_j^{(1,2)}(\alpha_{js}r)$	= Hankel function of the first or second kind
h	= hub radius
h_0	= blade spacing normal to the direction of the flow
i	= $\sqrt{-1}$
$J_{\pm}$	= split functions defined in Ref. 13
j	= integer indicating azimuthal mode order
$K_{js}^{\pm}$	= see Eq. (9)
$k_{js}^{\pm}$	= see Eq. (6)
k_0	= acoustic wave number ω/c_0
L	= scale of flow variation in spanwise direction
l	= spanwise length scale
M	= duct axial flow Mach number
M_e	= flow Mach number relative to the blade
n	= integer specifying blade number
$\boldsymbol{n}$	= unit normal to blade
P_n	= pressure fluctuations generated by blade boundary layer on nth blade
$p(\boldsymbol{x}, t)$	= acoustic pressure field
r, r_0	= duct coordinate; see Fig. 1
r_e	= distance of observer from trailing edge of isolated airfoil
S	= blade surface
$S_{FF}^{(n,m)}(\boldsymbol{y}, \boldsymbol{y}', \omega)$	= cross-spectral density of blade loadings on mth and nth blades
$S_{PP}(\omega)$	= spectrum of surface pressure fluctuations
$S_{ww}^{\pm}(\omega)$	= sound power in upstream or downstream direction (+ refers to upstream)
s	= integer indicating radial mode order
T	= averaging time
T_{ij}	= Lighthill's stress tensor
t	= observer time
U	= duct axial flow speed
U_c	= gust convection velocity
$U_j(\alpha_{js}r)$	= duct mode function
V	= source volume
$V_n(\boldsymbol{y}, \tau)$	= surface normal velocity
X_{js}	= constant defined in Eq. (15)
x	= chordwise location on a rectilinear blade
$x_i, \boldsymbol{x}$	= position vector
Y_{js}	= constant defined in Eq. (15)
y	= spanwise location on a rectilinear blade
$y_i, \boldsymbol{y}$	= position vector
z, z_0	= duct coordinate; see Fig. 1
α_{js}	= duct mode radial wave number
β	= blade angle; see Fig. 1
β_{js}	= duct mode axial wave number
Γ_{js}	= duct mode constant defined in Eq. (3)
γ_c	= ω_j/U_c
γ	= chordwise wave number
$\Delta\omega$	= frequency bandwidth
δ	= length scale of order boundary-layer thickness
ζ_c	= $(1-M_e^2)^{1/2}[\kappa_e^2-(\gamma_c+\kappa M_e)^2]^{1/2}$
$\zeta_{js}^{\pm}$	= see Eq. (6)
θ	= blade camber in Eq. (5)
κ	= $\omega_j/[c_0(1-M_e^2)]$
κ_e^2	= $\kappa^2-\nu^2/(1-M_e^2)$
μ	= $\sqrt{1-M^2}$
ν, ν_1	= spanwise wave number
ξ	= blade coordinate; see Fig. 1
ρ_0	= mean density
τ	= source time
ϕ, ϕ_0	= duct coordinate; see Fig. 1
ϕ_n	= blade coordinate; see Eq. (5)
$\Psi(\,)$	= see Eq. (18)
$\Psi_1(\,)$	= blade response function of isolated blade
Ω	= rotational speed of fan
ω	= frequency
ω_j	= $\omega - j\Omega$

Received May 9, 1997; presented as Paper 97-1612 at the AIAA/CEAS 3rd Aeroacoustics Conference, Atlanta, GA, May 12–14, 1997; revision received April 5, 1998; accepted for publication April 14, 1998.

*Professor, Center for Acoustics and Vibration, Department of Ocean Engineering. Senior Member AIAA.
†Graduate Student, Department of Ocean Engineering.

I. Introduction

BROADBAND noise from ducted fans has become an important issue in modern aeroengine design. Future concepts call for ultrahigh bypass ratio engines with large fans, which have lower rotational speeds than their predecessors. As a consequence, the

blade passage frequency of the fan is reduced to frequencies that are below the subjectively important part of the spectrum. In the past, the dominant contributor to the frequencies that determine the aircraft noise certification levels on approach was the fan tones, but this is no longer the case, and the high-frequency broadband noise from the fan is now thought to be of equal importance.[1]

Fan broadband noise is classified into two different categories: self-noise, which specifies the sound radiated by the self-generated turbulence close to the blade surfaces, and inflow noise, which is the sound radiated by the interaction of the blades with turbulence generated at some upstream location. The self-noise is the base level of the radiated sound field and is important because it represents the minimum achievable level of broadband noise from the fan. This paper will consider methods for predicting fan self-noise for ducted subsonic fans.

The self-noise from a ducted fan can be further broken down into two different source mechanisms. First there is blade boundary-layer noise, which is generated by the turbulence in the blade boundary layer interacting with the trailing edge and is sometimes referred to as trailing-edge noise. Second, there is tip flow noise, which is generated by the complicated flow around the blade tips and its interaction with the duct wall boundary layer. Little is known about tip flow noise, although experimental observations[2] have shown changes in fan noise with variations in tip gap dimensions. In contrast, a large amount of work has been done on trailing-edge noise for unducted rotors,[3–9] but the application of these concepts to ducted fans does not appear to have been studied. This paper will address this issue and apply the known concepts of trailing-edge noise to a ducted fan configuration, considering in particular the coupling of the trailing-edge noise source to the sound field in the fan duct.

Theoretical studies of trailing-edge noise[3–7] have shown that the source mechanism of trailing-edge noise is the scattering of sound at the sharp trailing edge of the blade. The sound is actually generated by the turbulence in the blade boundary layer, but because this is convected subsonically, it does not couple with the acoustic far field. However, it does generate a strong near field, which causes significant pressure fluctuations on the blade surfaces, and to ensure that the flow past the trailing edge is continuous, a viscous wake must be generated. It is the interaction of the sound generated in the boundary layer and the wake with the surface upstream of the trailing edge that causes waves to propagate to the acoustic far field. Analytical solutions to this problem can be posed in terms of a boundary value problem in which the Kutta condition is imposed at the trailing edge of the blade. Of particular relevance is the theoretical approach developed by Amiet,[6] who gives a formulation relating the far-field spectral level to the spectrum of the convected boundary-layer pressure fluctuations and their spanwise correlation length scale. Both factors need to be known to predict the sound from a ducted fan, and although it is possible to measure the surface pressure spectrum using pressure transducers embedded in the blade surface, it is very difficult to measure the spanwise correlation length scale. An alternative approach is to estimate the combination of these two parameters from acoustic far-field measurements of an isolated airfoil in a wind tunnel. By using Amiet's[6] relationship, measurements of the acoustic field can be inverted to obtain the components of the surface pressure spectrum, which are important for sound radiation. This approach has the advantage that nonradiating components of the surface pressure spectrum are correctly filtered out of the estimated surface pressure. A further advantage of this approach is that an extensive database exists[9] for the self-noise generated by isolated blades at different flow speeds and blade angles of attack. Consequently, by combining this data set with Amiet's theory, we can specify the blade surface parameters needed to compute trailing-edge noise.

In this study, we are interested in ducted fan blades, and so to predict the in-duct sound levels, we require the surface pressure spectrum and correlation length scales on the fan or stator blade surfaces. This information is not available but can, in the first instance, be estimated from the measurements on isolated blades as described earlier. However, ducted fan blades differ in many respects from the blades used in the study by Brooks et al.[9] First, fan blades are not isolated, and so the flow may be influenced by the presence of an adjacent blade. This can have an important effect on the acoustic scattering as will be discussed later, but its influence on the blade boundary-layer properties is not clear. The second difference is the blade camber. The measurements of Brooks et al.[9] are for uncambered blades, whereas typical fan designs have blades with significant camber. However, it is argued by Chase[5] that the boundary-layer properties scale with the flow speed and the boundary-layer momentum thickness at the blade trailing edge. Consequently, the results of Brooks et al.[9] can be used in principle for ducted fan blades providing a relationship is established that ensures that the blade trailing-edge boundary-layer properties are the same in each case.

Because fan blades are rotating, the flow speed and the angle of attack vary significantly across the span. However, the spanwise correlation length scale of typical boundary-layer flows may be assumed to be on the order of the boundary-layer thickness, and this is small compared with both the spanwise scale of the mean flow variables and the acoustic wavelength. This suggests that the boundary-layer properties of a rotating blade may be approximated by splitting the blade into spanwise strips and assuming the boundary layer is the same as that of a blade in rectilinear motion with the same local flow speed and angle of attack.[9] However, the surface pressure spectrum that couples with the acoustic field is correlated over a spanwise distance that is the order of the acoustic wavelength, and so this strip theory approach is only valid in the high-frequency limit where the acoustic wavelength is small compared with the blade span. This is a significant limitation, and the consequences of this approximation for the ducted fan configuration will be considered in Sec. II.

In Sec. II of this paper, a theory is developed for the sound power radiated from a ducted fan by trailing-edge noise sources. The turbulent boundary-layer fluctuations are assumed uncorrelated on each blade, but a correction is included for acoustic scattering from adjacent blades. The blade surface pressure spectrum is based on the interpolation of the measurements by Brooks et al.[9] on isolated airfoils. The scaling of the results as a function of the blade design parameters is given in Sec. III.

II. Evaluation of the In-Duct Sound Power for Trailing-Edge Noise

A. Theory for Noise from Blades Rotating in a Duct

In deriving a theory for the noise generated by ducted fan blades, we must consider the general problem of sound radiation from an unsteady flow over moving surfaces in a duct. This problem is illustrated in Fig. 1, which shows a set of fan blades in a circular duct and

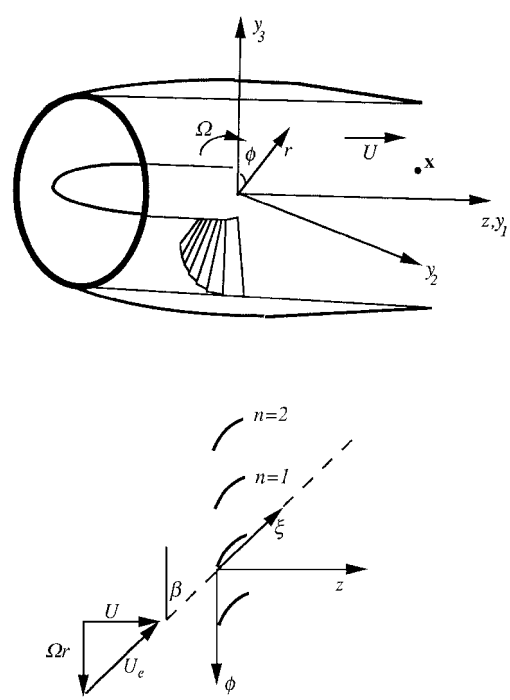

Fig. 1 Coordinate systems used in the analysis.

an observer at the location $\boldsymbol{x}$. By using Lighthill's acoustic analogy, the acoustic pressure at the observer can be specified as

$$p(\boldsymbol{x},t)=\int_{-T}^{T}\int_{V}T_{ij}(\boldsymbol{y},\tau)\frac{\partial^2 G(\boldsymbol{y},\tau\mid\boldsymbol{x},t)}{\partial y_i\partial y_j}\,\mathrm{d}V\,\mathrm{d}\tau + \int_{-T}^{T}\int_{S}f_i(\boldsymbol{y},\tau)\frac{\partial G(\boldsymbol{y},\tau\mid\boldsymbol{x},t)}{\partial y_i}\,\mathrm{d}S\,\mathrm{d}\tau + \int_{-T}^{T}\int_{S}\rho_0 V_n(\boldsymbol{y},\tau)\frac{D_0 G(\boldsymbol{y},\tau\mid\boldsymbol{x},t)}{D\tau}\,\mathrm{d}S\,\mathrm{d}\tau \tag{1}$$

where $G(\boldsymbol{y},\tau\mid\boldsymbol{x},t)$ is Green's function that applies for a source in the duct at $\boldsymbol{y}$ and an observer at $\boldsymbol{x}$ in accordance with the conventions given in Ref. 10. The first term on the right-hand side of this equation is the quadrupole source term, which represents the sound generated by the turbulent flow fluctuations. In the blade boundary layer, these sources are convected subsonically relative to both the observer and the rotor blades, and there is no rapid streamwise distortion of the flow, which can be assumed uniform at the trailing edge of the blades if the Kutta condition applies. The second term represents the dipole source term. The last term represents the contribution from the moving volume of the blade commonly referred to as thickness noise. This term is not important for ducted fans and only contributes to the near field at the blade passage frequencies, and so it will be ignored.

To evaluate the levels of trailing-edge noise, two different approaches have been used. Ffowcs Williams and Hall[3] and Howe[4] used a Green's function that satisfied the boundary conditions for a semi-infinite flat plate and so were able to eliminate the dipole term in Eq. (1). In Howe's approach,[4] a vorticity distribution is shed from the trailing edge to ensure that the Kutta condition is satisfied. In contrast, Amiet[6] specified a convected pressure disturbance on the surface of the blade that was induced by the quadrupole sources in the blade boundary layer. He then assumed that the turbulence in the boundary layer was undistorted as it convected past the trailing edge and introduced a correction to the local acoustic field, which ensured that there was no pressure discontinuity in the blade wake. In essence, both Howe's and Amiet's wake corrections are identical, the only difference being the manner in which the problem is set up. Howe specifies the flow explicitly, whereas Amiet specifies the net contribution of the induced flow in the wake. Both theories show that the subsonically convected turbulence in the boundary layer does not radiate to the acoustic far field and that no sound is radiated if the eddy convection velocity equals the freestream velocity. In the analysis given here, we will use Amiet's approach and define the acoustic field in terms of the blade surface pressure, ignoring the quadrupole term because this does not couple with the acoustic field. On this basis,[6] we need only consider the dipole term in Eq. (1).

Green's function can be defined for the acoustic field in a hard walled circular duct with a uniform axial flow[10] as

$$G(\boldsymbol{y},\tau\mid\boldsymbol{x},t)=\frac{i}{4\pi}\int_{-\infty}^{\infty}\sum_{j,s}\frac{U_j(\alpha_{js}r_0)}{\beta_{js}\Gamma_{js}}\times\exp\!\left[-i\omega\tau+ij\phi_0-i(Mk_0z_0\pm\beta_{js}z_0)\big/\mu^2\right]\times\left\{U_j(\alpha_{js}r)\exp\!\left[i\omega\tau-ij\phi+i(Mk_0z\pm\beta_{js}z)\big/\mu^2\right]\right\}\mathrm{d}\omega \tag{2}$$

where the observer is located at r_0, ϕ_0, z_0 and the source point is r, ϕ, z (z is in the direction of the flow, and the $\pm$ refers to an observer in the upstream/downstream direction). The axial flow Mach number is M and $\mu^2=1-M^2$. The wave number k_0 is defined as ω/c_0, where c_0 is the speed of sound, and the coefficients α_{js} are the solutions to $U_j'(\alpha a)=U_j'(\alpha h)=0$. We also have that

$$\beta_{js}=\sqrt{k_0^2-\mu^2\alpha_{js}^2}\qquad \Gamma_{js}=\pi\left\{\left[r^2-\left(j^2\big/\alpha_{js}^2\right)\right]U_j^2(\alpha_{js}r)\right\}_h^a \tag{3}$$

The terms in Eq. (2) have been arranged so that those that depend on the source coordinates are grouped in the braces. Consequently, when Eq. (2) is used in Eq. (1), we can carry out the integrals over the source variables separately and define a modal expansion for the acoustic field in the form

$$p(\boldsymbol{x},t)=\int_{-\infty}^{\infty}\sum_{j,s}A_{js}(\omega)U_j(\alpha_{js}r_0)\times\exp\!\left[ij\phi_0-i(Mk_0\pm\beta_{js})z_0\big/\mu^2-i\omega t\right]\mathrm{d}\omega \tag{4}$$

To obtain the mode amplitudes $A_{js}(\omega)$ for the dipole term in Eq. (1), we will first assume that the thickness of the blade is small compared with the acoustic wavelength,[10] and so the surface integral in Eq. (1) may be replaced by an integral over the blade planform, and the force applied to the fluid is replaced by the pressure jump across the blade. The integral over the planform must be carried out for each blade separately, and so we define $\boldsymbol{y}_n(\boldsymbol{r},\tau)$ as the location (in stationary coordinates) of the point $\boldsymbol{r}$ on the nth blade at time τ. In cylindrical coordinates, $\boldsymbol{y}_n=[r,\phi_n(r,z,\tau),z]$, where $z_u<z<z_D$ specifies the axial extent of the blades at each radial location. If we define ξ as the chordwise location on the mean blade planform (see Fig. 1) and β as the angle that the mean blade planform makes with the direction of rotation (so that $\tan\beta=U/\Omega r$), then $z-z_u=\xi\sin\beta$, and we can define

$$\phi_n=\Omega\tau-(2\pi n/B)-\xi\cos\beta/r-\theta(r,z) \tag{5}$$

where $\theta(r,z)$ defines the blade camber relative to the mean chord line.

The force applied to the fluid is in the direction normal to the blade surface, and so the gradient of Green's function in the dipole term of Eq. (1) must be evaluated in this direction. The normal is defined by $\boldsymbol{n}=\nabla g/|\nabla g|$ where $g=\phi-\phi_n$, and so if we define $F_n(r,\xi,\omega)$ as the Fourier transform with respect to time of the blade surface pressure fluctuations on the nth blade, the mode amplitudes will be

$$A_{js}(\omega)=\frac{1}{2\beta_{js}\Gamma_{js}}\sum_{n=1}^{B}\int_h^a\int_0^c\zeta_{js}^{\pm}U_j(\alpha_{js}r)F_n(r,\xi,\omega-j\Omega)\times\exp\!\left[ik_{js}^{\pm}\xi+2\pi inj/B+ij\theta(r,\xi)\right]\mathrm{d}r\,\mathrm{d}\xi/n_\xi \tag{6}$$

where

$$n_\xi=n_\phi\sin\beta+n_z\cos\beta$$

$$k_{js}^{\pm}=j\cos\beta/r+(Mk_0\pm\beta_{js})\sin\beta/\mu^2$$

$$\zeta_{js}^{\pm}=\frac{jn_\phi}{r}-\frac{(Mk_0\pm\beta_{js})n_z}{\mu^2}-\frac{\alpha_{js}U_j'(\alpha_{js}r)n_r}{U_j(\alpha_{js}r)}$$

Given the dimensions of the duct, all of the quantities in Eq. (6) are known apart from the blade loading distribution F_n. This result allows for blades with arbitrary shape, but it is often reasonable to ignore the effect of the blade camber, sweep, and lean on the amplitude terms in Eq. (6) by approximating the normal to the blade surface as

$$\boldsymbol{n}=(n_r,n_\phi,n_z)\approx(0,\sin\beta,\cos\beta) \tag{7}$$

The duct modes are useful because they can be used to calculate the in-duct sound power propagating either upstream or downstream from the fan. The expression for the autospectrum of the sound power is[10]

$$S_{ww}^{\pm}(\omega)=\mathrm{Re}\left\{\sum_{j,s}\frac{\omega\mu^4\beta_{js}\Gamma_{js}}{\rho_0\omega\pm\beta_{js}U^2}\frac{\pi}{T}\mathrm{Ex}\left[|A_{js}(\omega)|^2\right]\right\} \tag{8}$$

This is a relatively simple expression and allows the spectrum of the sound power to be obtained from the spectrum of the mode amplitudes. Note how no sound power is radiated when β_{js} is imaginary, which eliminates the cutoff modes from the calculation.

The in-duct sound power generated by broadband noise sources is therefore given by the expected value of the mode amplitudes as a function of frequency. These can be defined from Eq. (6) in the form

$$\frac{\pi}{T}\mathrm{Ex}\left[|A_{js}(\omega)|^2\right] = \left(\frac{1}{2\beta_{js}\Gamma_{js}}\right)^2 \times \sum_{n=1}^{B}\int_h^a \sum_{m=1}^{B}\int_h^a \zeta_{js}^{\pm}(r)\zeta_{js}^{\pm}(r')U_j(\alpha_{js}r)U_j(\alpha_{js}r') \times \int_0^c\int_0^c S_{FF}^{(n,m)}(\boldsymbol{y},\boldsymbol{y}',\omega_j)\exp[iK_{js}^{\pm}(\xi,r) - iK_{js}^{\pm}(\xi',r') + 2\pi ij(n-m)/B]\,\mathrm{d}r\,\mathrm{d}r'\,\mathrm{d}\xi\,\mathrm{d}\xi'/n_\xi n'_\xi \tag{9}$$

where $\omega_j = \omega - j\Omega$ and $K_{js}^{\pm} = k_{js}^{\pm}\xi + j\theta(r,\xi)$. The term $S_{FF}^{(n,m)}$ is the cross-spectral density of the pressure fluctuations on blades number m and n at the locations $\boldsymbol{y} = (r,\xi)$ and $\boldsymbol{y}' = (r',\xi')$, which is defined as

$$S_{FF}^{(n,m)}(\boldsymbol{y},\boldsymbol{y}',\omega_j) = (\pi/T)\mathrm{Ex}\left[F_n(r,\xi,\omega_j)F_m^*(r',\xi',\omega_j)\right] \tag{10}$$

If the fluctuations on each blade are uncorrelated, then only those terms for which $n = m$ need be included in the summations, but in general that will not be the case because the blades are coupled by the acoustic field.

This result shows that the acoustic field depends on the cross spectrum of the blade loading distribution, and this must be known with sufficient accuracy to calculate the surface integral in Eq. (9). Note that the integrand also includes highly oscillatory functions, and the coupling of these to the cross spectrum is crucial to the accuracy of the result.

The blade loadings for broadband sources on rotating blades are not well understood. At the present time, the fully coupled blade response to either an unsteady inflow or a turbulent boundary layer can only be obtained numerically,[11,12] and calculations to date have been limited to the first few blade passage harmonics. Broadband noise calculations are an order of magnitude more difficult because they require multiple frequency calculations at very high frequencies. Therefore we are limited at this time to estimating the blade response function for a rotating blade by using the blade response functions for rectilinear blades applied to incremental strips across the span. The accuracy of this approximation depends on the spanwise extent of the blade response to a local excitation. In broadband noise calculations, it is often argued that the spanwise correlation length scale of the incident fluctuations is small, and so each spanwise strip of the blade can be considered uncorrelated.[6] However, this argument only applies to the flow exciting the blade and does not consider the blade response, which may effectively spread the influence of a local gust across the blade span. In the following sections, we will examine this approximation for trailing-edge noise sources on a rotating blade.

B. Blade Surface Pressure

The theory for trailing-edge noise from an isolated blade can be found in Ref. 6 where it is shown that the acoustic radiation depends on both the turbulent boundary-layer pressure fluctuations and the blade response function. In fan noise applications, the blade response function also depends on the acoustic scattering by adjacent blades. This problem was studied for a linear cascade model in Ref. 13, and significant blade-to-blade interactions were identified. In this section, we will review the results of Ref. 13 so that they may be used for the evaluation of Eq. (9).

It will be assumed that the pressure fluctuations generated by the blade boundary layer far upstream of the trailing edge of the nth blade can be represented by

$$P_n(y,x,\tau) = \int_{-\infty}^{\infty}\int_{-\infty}^{\infty} P_n(\omega_j,\nu)\exp[i\nu y - i\omega_j\tau + i\gamma_c x]\,\mathrm{d}\nu\,\mathrm{d}\omega_j \tag{11}$$

(Note that this formulation differs from that given in Ref. 6 in as much as the response is allowed to be a function of span.) The blade loading on a rotor blade will depend on both the boundary-layer fluctuations on the excited blade as well as those on the adjacent blades, and so in the presence of the trailing edge, the loading can be written in the form

$$F_n(y,x,\omega_j) = \sum_{k=1}^{B}\int_{-\infty}^{\infty} g_{n-k}(x,\nu,\omega_j)P_k(\omega_j,\nu)e^{i\nu y}\,\mathrm{d}\nu \tag{12}$$

The function g_{n-k} is the blade response function of the nth blade to a boundary layer on the kth blade. The cross spectrum of the surface pressure required in Eq. (9) will therefore depend on $\mathrm{Ex}[P_n(\omega_j,\nu)P_m^*(\omega_j,\nu')]$, which can be evaluated for a homogeneous turbulent boundary layer that is uncorrelated from blade to blade but has the same average properties, as

$$\frac{\pi}{T}\mathrm{Ex}\left[P_n(\omega_j,\nu)P_m^*(\omega_j,\nu')\right] = \frac{lS_{PP}(\omega_j)}{\pi}\delta(\nu-\nu')\delta_{mn} \tag{13}$$

where $S_{PP}(\omega_j)$ is the spectrum of the surface pressure fluctuations at a point. The parameter l is the spanwise length scale as defined by Amiet,[6] which is a function of the spanwise wave number. It is often argued that the dependence of l on the spanwise wave number can be ignored because it is only important when $\nu\delta > 1$, where δ is a length scale that is on the order of the boundary-layer thickness, but we will not make this approximation until a later stage. We then obtain the cross spectrum of the blade loadings as

$$S_{FF}^{(n,m)}(\boldsymbol{y},\boldsymbol{y}',\omega_j) = \frac{S_{PP}(\omega_j)}{\pi}\sum_{k=1}^{B}\int_{-\infty}^{\infty} l g_{n-k}(x,\nu,\omega_j) \times g_{m-k}^*(x',\nu,\omega_j)\exp[i\nu(y-y')]\,\mathrm{d}\nu \tag{14}$$

The result given by Eq. (14) provides the cross spectrum of the loadings for a linear cascade that has uniform spanwise properties. By using strip theory, we can use this result as an input to Eq. (9) to obtain the amplitude of the duct modes in terms of the surface pressure spectrum S_{PP}.

C. Duct Mode Amplitudes Obtained from Strip Theory

The mode amplitudes defined by Eq. (9) can only be evaluated if the cross spectrum of the loadings are known, and as stated earlier, we will estimate these from the cross spectrum of the loadings on a linear cascade of semi-infinite flat plates with uniform flow at all spanwise locations. This is at best a high-frequency approximation because the properties of the boundary layer on the rotating blade will vary significantly across the span, and we must therefore use broadband strip theory to relate the linear cascade blade response to the rotating blade response. The assumption required is that $S_{FF}^{(n,m)}$ will tend to zero when the spanwise displacement $r - r'$ is greater than some distance L over which the flow conditions may be assumed constant. The blade response extends the influence of any locally excited region over a blade surface area that scales with the acoustic wavelength. Consequently, strip theory only applies when $kL \gg 1$. On this basis, we can carry out a local expansion of the Bessel function terms in Eq. (9), which retains the phase variation of Green's function across the span but relates all amplitude variations that depend on r' to their value at r. The expansion takes the form

$$\zeta_{js}^{\pm}(r')U_j(\alpha_{js}r') \approx \frac{\zeta_{js}^{\pm}(r)}{2}X_{js}H_j^{(1)}(\alpha_{js}r)\exp[i\nu_1(r-r')] + \frac{\zeta_{js}^{\pm}(r)}{2}Y_{js}H_j^{(2)}(\alpha_{js}r)\exp[-i\nu_1(r-r')] \tag{15}$$

where

$$U_j(\alpha_{js}r) = \tfrac{1}{2}X_{js}H_j^{(1)}(\alpha_{js}r) + \tfrac{1}{2}Y_{js}H_j^{(2)}(\alpha_{js}r)$$

This allows an approximation of the integrand of Eq. (9) in the vicinity of r so that it may be written (assuming uncambered blades aligned with the flow)

$$\frac{\pi}{T}\mathrm{Ex}\left[|A_{js}(\omega)|^2\right] = \left(\frac{1}{2\beta_{js}\Gamma_{js}}\right)^2 \int_h^a \int_{r-L}^{r+L} \left[\zeta_{js}^{\pm}(r)\right]^2 \frac{U_j(\alpha_{js}r)}{2}$$
$$\times \left\{X_{js}H_j^{(1)}(\alpha_{js}r)\exp[i\nu_1(r'-r)] + Y_{js}H_j^{(2)}(\alpha_{js}r)\right.$$
$$\left.\times \exp[-i\nu_1(r'-r)]\right\} \sum_{n=1}^{B}\sum_{m=1}^{B} \int_0^c \int_0^c S_{FF}^{(n,m)}(\mathbf{y},\mathbf{y}',\omega_j)$$
$$\times \exp\left[ik_{js}^{\pm}(\xi-\xi') + 2\pi ij(n-m)/B\right] \mathrm{d}r\,\mathrm{d}r'\,\mathrm{d}\xi\,\mathrm{d}\xi' \qquad (16)$$

In approximating Eq. (9) using Eq. (16), we have introduced an important simplification of the broadband noise problem from rotating blades because it allows us to substitute S_{FF} from Eq. (14) directly using the local flow conditions at the spanwise station r. Evaluating the integrals using Eq. (14) with $y - y' = r - r'$ and $x = \xi - c$ in the strip theory limit $kL \gg 1$ gives

$$\frac{\pi}{T}\mathrm{Ex}\left[|A_{js}(\omega)|^2\right] = \left(\frac{1}{2\beta_{js}\Gamma_{js}}\right)^2 B\int_h^a \left[\zeta_{js}^{\pm}(r)U_j(\alpha_{js}r)\right]^2$$
$$\times 2lS_{PP}(\omega_j, r)\left|\Psi\left(\omega_j, \nu_1, k_{js}^{\pm}\right)\right|^2 \mathrm{d}r \qquad (17)$$

where

$$\Psi\left(\omega_j, \nu_1, k_{js}^{\pm}\right) = \sum_{n=1}^{B}\int_0^c g_n(\xi - c, \nu_1, \omega_j)\exp\left[ik_{js}^{\pm}\xi + 2\pi ijn/B\right]\mathrm{d}\xi$$

Note that we have used the property $g_{-n} = g_{B-n}$ and given S_{PP} a dependence on r to indicate that it is a function of spanwise location. Also we have taken g_n to be an even function of the spanwise wave number, which is to be expected in the uniform flow approximation. This result shows how the duct mode amplitudes are dependent on the surface pressure spectrum S_{PP}, the blade response function Ψ, and the spanwise length scale l. The blade response function can be defined analytically, but the surface pressure and the spanwise length scale are features of the flow that are hard to predict or to determine from computations of the flow. Typically we are interested in blades that are operating close to stall, and so the flow is very unstable, and nonlinear interactions are important. At this time, we are limited to estimating the surface pressure from experiments on isolated blades and interpolating the results to the conditions of interest. This approach will be described in Sec. II.F.

D. Phase Approximation

To obtain the result given by Eq. (17), it was necessary to make use of the local expansion, Eq. (15), and in this section, we will evaluate the value of the phase function ν_1. First consider a Taylor series expansion of the Hankel function in Eq. (15). This may be written in the form

$$H_j^{(1)}(\alpha r') = \exp\left\{\ell n\left[H_j^{(1)}(\alpha r)\right] + (r'-r)\frac{\partial}{\partial r}\left(\ell n\left[H_j^{(1)}(\alpha r)\right]\right)\right\} \qquad (18)$$

so that we can define the phase function as

$$\nu_1 = -i\frac{\partial}{\partial r}\left(\ell n\left[H_j^{(1)}(\alpha r)\right]\right) = \frac{-i\alpha H_j'^{(1)}(\alpha r)}{H_j^{(1)}(\alpha r)} \qquad (19)$$

For large values of the argument, we can approximate the Hankel function as

$$H_j^{(1)}(\alpha r) = \sqrt{\frac{2}{\pi\alpha r}}\exp\left[i\left(\alpha r + \frac{4j^2-1}{8\alpha r} - j\pi/2 - \pi/4\right)\right] \qquad (20)$$

so that

$$\nu_1 = \alpha - \frac{4j^2-1}{8\alpha r^2} + \frac{i}{2r} \qquad (21)$$

We see therefore that the real part of the phase function depends on the radius, and although this dependence is weak well above cutoff, there is an implicit radial dependence.

One of the problems with using a flat plate blade response function to represent a blade rotating in a cylindrical duct is the matching of the response at frequencies where the duct modes cut on. At the cut-on frequency, $\beta_{js} = 0$, and so considering Eqs. (8) and (9), we see that the sound power of each mode is singular at cut-on. However, for a rectilinear cascade, it can be shown that the blade response function tends to zero at the cut-on frequency,[10] and so the sound power remains finite. It is therefore important that, when modeling the response of the rotating blade by an equivalent rectilinear blade over a finite strip (however small), the behavior at cut-on is correct. This is especially significant for broadband noise calculations because at high frequencies the modal density in any bandwidth of practical interest is high, and so there will be several modes that cut on within any band. The singular behavior of the expressions for the sound power and the mode amplitudes can cause large errors unless it is accounted for correctly.

To address this problem, consider the dispersion relationship for acoustic waves in cylindrical coordinates. For a wave field in a duct with uniform flow in the axial direction, the acoustic pressure is given by $p = AU_j(\alpha_{js}r)\exp(-i\omega t + ij\phi + i\gamma z)$. The dispersion relationship that determines γ is given by

$$\gamma^2 + \alpha_{js}^2 = \frac{(\omega - \gamma U)^2}{c_0^2} \qquad (22)$$

In contrast, the acoustic field in rectilinear coordinates with a uniform flow in the z direction is defined as $p = A\exp(-i\omega t + i\nu y + i\beta x + i\gamma z)$ and satisfies the dispersion relationship

$$\gamma^2 + \beta^2 + \nu^2 = \frac{(\omega - \gamma U)^2}{c_0^2} \qquad (23)$$

If the x axis is aligned with the azimuthal direction so that $x = \phi r$, the periodicity of the wave field requires that $\beta = j/r$. Consequently, the dispersion relationships will be identical if

$$\nu^2 = \alpha_{js}^2 - (j^2/r^2) \qquad (24)$$

To first order, we can expand this relationship to give

$$\nu = \alpha_{js} - \frac{j^2}{2\alpha_{js}r^2} \qquad (25)$$

which is a good approximation to the Taylor series expansion given by Eq. (21). The difference between Eqs. (19) and (24) is illustrated in Fig. 2 for different mode orders. The results have only been plotted for a duct with no centerbody for values of $\alpha_{js}r > \alpha_{j1}r$, which corresponds to the cut-on modes. We see from this result that the approximation is good for the higher-mode orders and is worst for the lowest-order mode close to the cut-on location.

In conclusion, when aligning the wave numbers in rectilinear coordinates with the wave numbers in cylindrical coordinates, it is important that the dispersion relationships are preserved so that the cut-on frequencies for each mode are the same in both cases. For this reason, we must choose the spanwise wave number given by Eq. (24) in the rectilinear expansion, and this gives a good approximation for the local expansion of the Bessel functions.

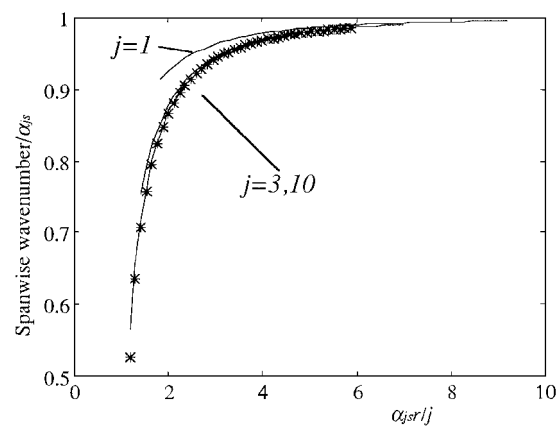

Fig. 2 Evaluation of radial phase approximation ∗ is the approximation given by Eq. (24), and the lines show Eq. (19) for different mode orders.

E. Blade Response Function

The blade response function for pressure fields convected past the trailing edges of a linear cascade of blades was investigated in Ref. 13, where it was shown that, for an incident pressure field of the type given by Eq. (11),

$$g_n(x, \nu, \omega_j) = \int_{-\infty}^{\infty} \exp[-i\gamma(x - nd)] \times \sum_{p=-\infty}^{\infty} A_p(\gamma, \nu) \exp\left(\frac{-2\pi ipn}{B}\right) d\gamma \tag{26}$$

where the function A_p is defined by Eq. (23) of Ref. 13 [with $Q \exp(i\xi_0|y_0|) = \frac{1}{2}$ to account for pressure doubling on the surface], and the trailing edge of each blade lies at $x = nd$. It then follows that the function required in Eq. (17) is given by

$$\Psi(\omega_j, \nu, \gamma) = 2\pi B e^{i\gamma c} \sum_{p=-\infty}^{\infty} A_{j-pB}(\gamma, \nu) \tag{27}$$

and by combining Eqs. (23), (26), and (28) of Ref. 13, we find that

$$\Psi(\omega_j, \nu, \gamma) = \frac{i\zeta_c e^{i\gamma c}}{4\pi i(\gamma + \gamma_c) J_+^{(j)}(-\gamma_c) J_-^{(j)}(\gamma)} \tag{28}$$

where $\zeta_c = (1 - M_e^2)^{1/2}[\kappa_e^2 - (\gamma_c + \kappa M_e)^2]^{1/2}$, $\kappa_e^2 = \kappa^2 - \nu^2/(1 - M_e^2)$, $\kappa = \omega_j/c_0(1 - M_e^2)$, and $\gamma_c = \omega_j/U_c$. This result is only valid for calculating the sound field in the region downstream of the blade trailing edges because the model used is for a cascade of blades with semi-infinite chord. For the sound that propagates in the upstream direction, the sound field is trapped in the blade passages and then radiates from the inflow plane of the fan. A complete theory for the propagation of waves through the blade passages, their reflection, and subsequent radiation is not yet available, but current indications are that there is very little energy reflected back downstream from the fan leading edge.

To interpret the results it is shown in Ref. 13 that a reasonable approximation is given for Eq. (28) in the form

$$\Psi(\omega_j, \nu, \gamma) = \frac{(1 - e^{2i\zeta h_0})e^{i\gamma c}}{i(\gamma + \gamma_c)} \sqrt{\frac{\kappa_e + \gamma_c + \kappa M_e}{\kappa_e - \gamma + \kappa M_e}} \tag{29}$$

where $\zeta = (1 - M_e^2)^{1/2}[\kappa_e^2 - (\gamma - \kappa M_e)^2]^{1/2}$. Two features are important about this result. First, the term $[1 - \exp(2i\zeta h_0)]$ represents the reflection of waves by adjacent blades and is typical of an interference effect. The response function therefore has zeros at frequencies where $\zeta h_0 = \pi$, and these will be apparent in the computation of the sound power spectra to be discussed in Sec. III. Second, the function given in Eq. (29) reduces to the blade response function for an isolated blade in the limit that h_0 tends to infinity because ζ has a small positive imaginary part so that $[1 - \exp(2i\zeta h_0)] \sim 1$.

F. Surface Pressure Spectrum

To evaluate the spectrum of the blade boundary-layer pressure fluctuations, we will consider measurements of the acoustic field from an isolated blade. It is shown in Ref. 6 that the far-field pressure spectrum from an isolated blade in a uniform flow is given in terms of the cross spectrum of the blade pressure fluctuations. To evaluate Eq. (17), we need to specify $2lS_{PP}$, and this can be determined from the measurement of the pressure spectrum in the acoustic far field as

$$2lS_{PP}(\omega_j) = \frac{S_{PP}(\boldsymbol{x}_0, \omega_j)}{(\omega_j/4\pi c_0 r_e)^2 b|\Psi_I(\omega_j, 0, \kappa M_e)|^2} \tag{30}$$

where Ψ_I is the blade response function of an isolated blade and we have specified the observer to be located at $x_0 = y_0 = 0$. It is therefore relatively simple to obtain the pressure spectrum required for Eq. (17) from measurements of the acoustic field from an isolated blade. The accuracy of this estimate is determined by the knowledge of the blade response function, but this is specified theoretically, and the primary assumption is that scattering by the leading edge of the blade is ignored.

G. Numerical Implementation

The theory described earlier has been implemented by carrying out five separate tasks based on the input parameters of a particular fan design.

1) The self-noise source spectra are calculated using the blade self-noise prediction code provided by Brooks et al.[9] This calculation is carried out for each blade station and gives spectral levels between 200 and 40,000 Hz in blade-based coordinates.

2) The duct mode eigenvalues and eigenfunctions are calculated for each frequency at each radial station with sufficient resolution for the radial integration required in Eq. (17).

3) The blade response function and source level are calculated for all cut-on modes at ~10 radial stations across the blade span.

4) The radial integration is carried out numerically. The mode functions are highly oscillatory, and so a small step size is required in the integration to define these correctly. Accurate results are obtained by using at least 30 steps across the span for the lower-order modes and by increasing this to $(a - h)/(5s_{\max})$ for large radial mode orders where $s_{\max}$ is the largest value of s for all propagating modes at a given frequency. However, relatively few source points are defined in task 3, but they tend to vary smoothly so that linear interpolation can be used to specify these functions at the small increments required for the mode functions.

5) The sound power is evaluated for each frequency and each mode using Eq. (17).

Numerical checks have been carried out on the radial integration by comparing the results with known theoretical solutions. Further checks on the number of radial stations required in task 3 have shown that 10 radial stations give a converged solution. The codes for the blade response function have been checked using the two alternate methods of calculation.

III. Results and Discussion

A. Numerical Examples

In this section, we will illustrate the application of the self-noise model described earlier to a ducted fan. We will limit consideration to a fan in a duct of radius 0.2286 m with 20 blades and a hub-to-tip ratio of 0.44. The results will be presented in terms of the spectrum level of the sound power obtained from Eq. (8) and corrected for the bandwidth used in the frequency analysis by multiplying by $2\Delta\omega$ with $\Delta\omega = 2\pi$ rad/s. Unless otherwise stated, the tip Mach number will be 0.7, the tip inflow angle $\beta = \tan^{-1}(U/\Omega a) = 23$ deg, and the blade chord 0.081 m. Two different distributions of blade angle of attack will be considered: a constant angle of attack of 7 deg at all spanwise locations and a varying angle of attack in which there is a linear reduction of blade angle from 8 deg at the hub to 4 deg at the tip.

B. Self-Noise Source Levels

The self-noise source levels are obtained from the nondimensionalized measured spectra given by Brooks et al.[9] for a series of NACA 0012 airfoils with different chords and at different angles of attack. The measured spectra in Ref. 9 scale with the fifth power of the inflow velocity, and significant increases in the low-frequency part of the spectrum were observed at high angles of attack when flow separation and/or stall occurred. Flow separation was significantly altered by the use of boundary-layer trips, indicating that significant scale effects may be present.

This study is concerned with high-solidity fans in which the local flow in a blade passage may vary significantly from a flow with the same Reynolds number over an isolated blade. In particular, the influence of adjacent blades on flow separation and boundary-layer development may be significant. Furthermore the airfoils used in the study of Brooks et al.[9] were uncambered, whereas ducted fan blades usually include a significant amount of camber. The relationship between the angle of attack of an isolated blade and the equivalent angle of attack of the blades in a high-solidity fan is yet to be determined and will require an extensive experimental study. However, results to date suggest that the blade incidence angles are equivalent between these two cases, but further work needs to be done to confirm this preliminary conclusion.

Figure 3 shows the isolated blade self-noise spectra for each radial station of the constant-angle-of-attack case (case A) described earlier. Note how the highest levels occur near the blade tip where

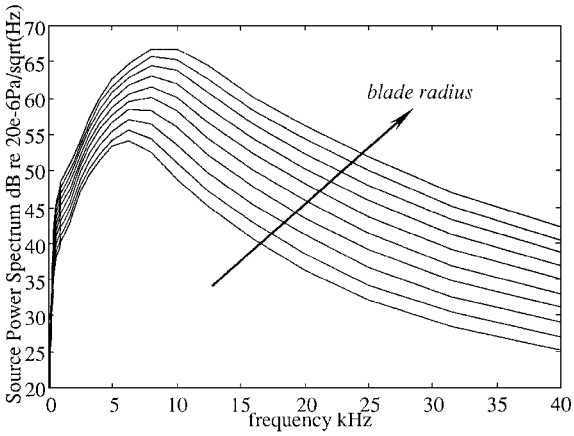

Fig. 3 Source spectra for a rotating blade with a constant angle of attack of 7 deg.

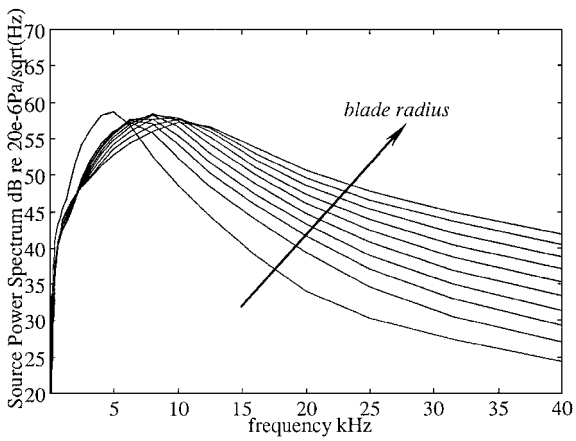

Fig. 4 Source spectra for a rotating blade with a linearly varying angle of attack from 8 deg at the hub to 4 deg at the blade tip.

the blade relative velocity is highest and how the spectral peak occurs at ~9000 Hz. At inboard stations, the peak moves to lower frequencies, and the levels are reduced as the fifth power of the blade relative velocity.

For the case when the blade angle of attack varies across the span (case B, Fig. 4), a different characteristic is observed. The increase in angle of attack on the inboard stations of the blade causes the level of the spectral peak to remain constant in spite of the reduction in blade relative velocity. This characteristic is caused by the flow over the blade approaching separation and will be affected by the details of the fan design. In general, we can conclude that separated flow will result in significant increases in low-frequency self-noise from the fan.

C. In-Duct Sound Power

To demonstrate the effect of the two different variations of blade angle of attack on the radiated power levels, Fig. 5 shows the downstream sound power for the blade source levels given in Figs. 2 and 3. Note how the constant-angle-of-attack case has higher levels, especially at high frequencies. The high-frequency characteristic is explained by the higher angle of attack close to the blade tip for case A. In contrast, the high angle of attack close to the hub causes blade stall for case B, and this results in higher low-frequency levels, as expected from Fig. 4.

An interesting feature is the noticeable dips in the spectra at ~8 kHz. This is caused by the interference effect discussed in Sec. II.E and is a direct consequence of the cascade blade response function having a null in this frequency band.

The scaling with Mach number is shown in Fig. 6 for case A, giving results for blade tip Mach numbers of 0.5, 0.6, 0.7, 0.8, and 0.9. To obtain these curves, the fan speed was varied while the same inflow angle and angles of attack were maintained. An

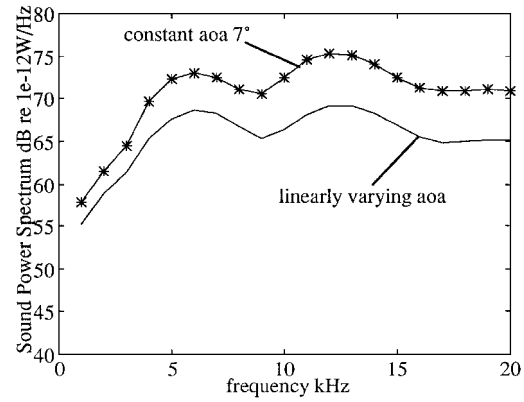

Fig. 5 Downstream sound power for an angle of attack that is a) constant across the span and b) linearly varying across the span.

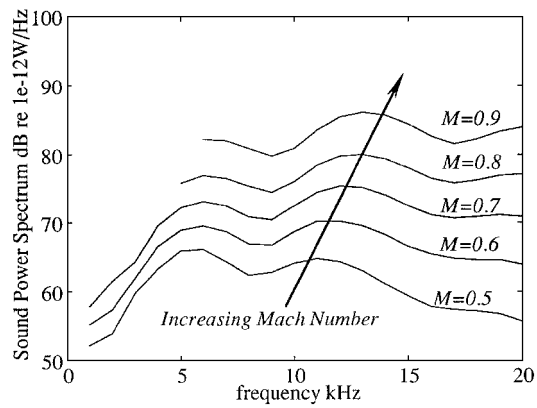

Fig. 6 Effect of increasing the Mach number on the downstream sound power for case A.

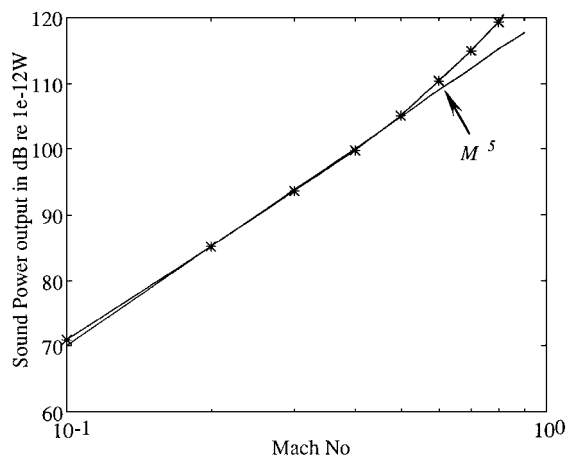

Fig. 7 Overall sound power for case A as a function of blade tip relative Mach number. (Note that for Mach numbers >0.7 levels are underestimated.)

increase in the spectral level is observed with greater increases at higher frequencies. To determine the scaling of self-noise with Mach number, Fig. 7 shows the total sound power as a function of blade tip Mach number obtained by integrating the spectra. For Mach numbers less than 0.5, the scaling is proportional to the fifth power of the Mach number as expected from the source levels. At higher Mach numbers, a greater sensitivity is observed, and the scaling is closer to the sixth power of the Mach number or greater. Note that at Mach numbers greater than 0.7 the complete spectra could not be calculated, and so the levels are obtained by integrating the available data shown in Fig. 5.

The scaling with angle of attack is shown in Fig. 8 for case A with nominal angle-of-attack changes of -2, -1, 0, $+1$, $+2$ deg

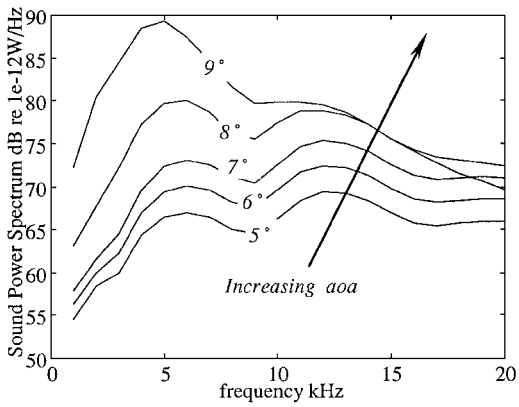

Fig. 8 Effect of increasing the angle of attack on the downstream sound power for case A.

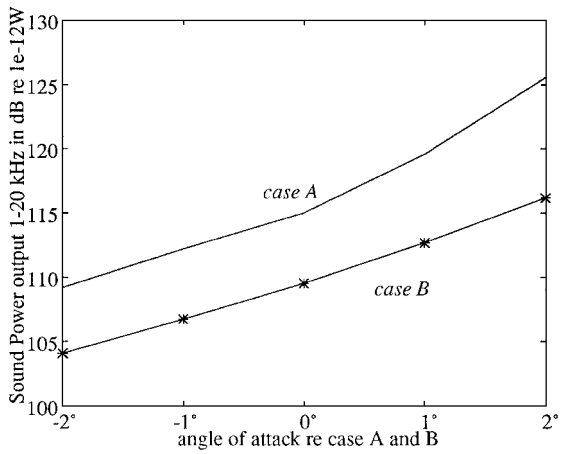

Fig. 9 Effect of increasing the angle of attack on the downstream overall sound power for cases A and B.

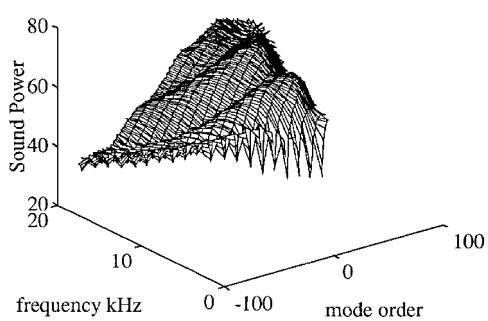

Fig. 10 Modal distribution of sound power as a function of frequency.

relative to the base level. Note here how the spectral shape changes significantly at low frequencies when blade stall occurs. In Fig. 9, the total sound power between 1 and 20 kHz is shown as a function of angle of attack for both cases A and B, and it is seen that this increases as ~2.4 dB/deg for case B, which has a twisted blade for which only the hub stalls in this range of parameters. Case A, which has a constant angle of attack across the span, shows more sensitivity because both the tip and the hub region stall at incidence angles greater than 7 deg.

D. Modal Power Distribution

One of the interesting features of the approach given here is that the distribution of sound power in each mode as a function of frequency can be displayed as shown in Fig. 10 for the constant-angle-of-attack case (case A). In this plot, the sound power is presented for all the azimuthal modes (x axis), against frequency (y axis), and the contour height (z axis) represents the sound power that is the sum of the levels in the radial modes. The plot shows a clear tendency for

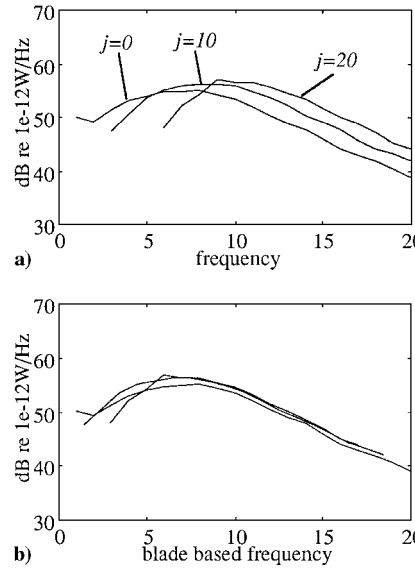

Fig. 11 Modal sound power for case A as a function of frequency and blade-based frequency for modes 0, 10, and 20.

there to be more sound power in the positive (corotating) modes at high frequencies, and at low frequencies there is more sound power in the negative (counter-rotating) modes. Figure 10 also highlights valleys in the modal power distribution that are caused by the blade-to-blade interference effects discussed in Sec. II.E.

To further investigate why the modal power is concentrated in the corotating modes, we note that the frequency-dependent factors that affect the mode strength given by Eq. (17) are the wave numbers β_{js} and $k_{js}^{\pm}$, the source spectrum $2lS_{PP}$, and the blade response function Ψ. The source spectrum and the blade response function are both functions of $\omega_j = \omega - j\Omega$, which represents the blade-based frequency and accounts for the Doppler shift of the moving blades by coupling different source frequencies into different duct modes. The interference effects due to blade-to-blade interactions that cause the valleys in Fig. 10 make it hard to separate out the source spectrum scaling for each mode, and so calculations were carried out using a blade response function that eliminated adjacent blade interference. This was achieved by letting h_0 tend to infinity in Eq. (29). The sound power spectra for the modes $j = 0$, 10, and 20 are shown in Fig. 11a. The spectral peak occurs at higher frequencies for the higher-order modes, but when plotted against the blade-based frequency (Fig. 11b), all the spectral peaks line up, showing that the sound power is primarily a function of the blade-based frequency. The match is not perfect at the lower frequencies because of the influence of the blade response function close to cut-on, and this is even more pronounced for negative mode orders, for which the spectral peak of the zero-order mode is cut off, but the high-frequency parts of the spectra line up as a function of the blade-based frequency.

IV. Conclusions

A theoretical prediction method for the broadband self-noise from ducted fans has been developed. The source mechanism is assumed to be the interaction of the turbulent boundary layer with the trailing edges of the blades, and the source levels are obtained from the measurements of self-noise from isolated blades.

It was shown that strip theory must be used to apply these results to a rotating blade, and this is only a valid approximation in the high-frequency limit where the acoustic wavelength is much smaller than the duct radius. A method was introduced for coupling the modes in a circular duct to the modes of a linear cascade. This is achieved by matching the dispersion relationship of the acoustic field in each case, and if this is not done correctly, then the incorrect behavior of the blade response function is obtained close to cutoff. This is important due to the singular nature of the expression for the sound power at the cutoff frequency.

It has been found that for a high-solidity ducted fan the blade surface pressures are not uncorrelated on each blade, and corrections

must be included for the scattering from the trailing edges of adjacent blades. This is achieved by using a blade response function that assumes blades of semi-infinite chord arranged as a linear cascade, and this function has the correct behavior to properly calculate the modes close to cutoff, which is not the case for approximate methods that do not include the effect of the spanwise wave number. However, a correction needs to be added to account for the propagation of trailing-edge noise through the blade passages and into the duct upstream of the fan.

Numerical results show that the in-duct sound power scales with the fifth power of the fan speed at low Mach numbers, but this changes to the sixth power or greater at high Mach numbers. The angle of attack of the blade increases the self-noise as 2.4 dB/deg, and significant increases in low-frequency self-noise occur if blade stall occurs. For blades with a linear variation of angle of attack, stall effects occur primarily in the hub region, and this does not give as large increases as do stall effects that occur in the tip region of the fan. It is also shown that the sound power is concentrated in the corotating modes because of the Doppler shift introduced by the fan.

The advantage of the approach given here is that it is based on an experimental database and so includes the effects of nonlinear source mechanisms and viscosity in high-Reynolds-number flows. Given the limitation that the flow is modeled as being the same as that of an isolated blade, the method makes a first-order attempt to account for the self-noise from blades at high angles of attack where separated flow and blade stall takes place over different sections of the blade. Clearly more work is required, both experimentally and numerically, to evaluate the turbulent boundary layer close to the trailing edge of fan blades that, in contrast to the blades used here, may be highly cambered and influenced by the presence of adjacent blades. However, the method described here should give a first-order estimate of the trailing-edge noise from a ducted fan.

Acknowledgments

This work was supported by NASA Grant NAG 1-1202. The authors would also like to thank T. F. Brooks for providing a copy of the self-noise prediction code that was used for the calculations presented in this report. Also, the authors would like to thank A. LaVigne, who helped with the numerical verification of the results.

References

[1]Gliebe, P. R., "Fan Broadband Noise—The Floor to High Bypass Engine Noise Reduction," *Proceedings of Noise Con 96*, Seattle, WA, Sept. 1996.

[2]Mugridge, B. D., and Morfey, C. L., "Sources of Noise in Axial Flow Fans," *Journal of the Acoustical Society of America*, Vol. 51, No. 5, 1972, pp. 1411–1426.

[3]Ffowcs Williams, J. E., and Hall, L. H., "Aerodynamic Sound Generation by Turbulent Flow in the Vicinity of a Scattering Half Plane," *Journal of Fluid Mechanics*, Vol. 40, 1970, pp. 657–670.

[4]Howe, M. S., "A Review of the Theory of Trailing Edge Noise," *Journal of Sound and Vibration*, Vol. 61, No. 3, 1978, pp. 437–465.

[5]Chase, D. M., "Sound Radiated by Turbulent Flow off a Rigid Half-Plane as Obtained from a Wavevector Spectrum of Hydrodynamic Pressure," *Journal of the Acoustical Society of America*, Vol. 52, No. 3, 1972, pp. 1011–1023.

[6]Amiet, R. K., "Noise Due to Turbulent Flow Past a Trailing Edge," *Journal of Sound and Vibration*, Vol. 47, No. 3, 1976, pp. 387–393.

[7]Kim, Y. N., and George, A. R., "Trailing-Edge Noise from Hovering Rotors," *AIAA Journal*, Vol. 20, No. 9, 1982, pp. 1167–1174.

[8]Brooks, T. M., and Hodgson, T. H., "Trailing Edge Noise Prediction from Measured Surface Pressures," *Journal of Sound and Vibration*, Vol. 78, No. 1, 1981, pp. 69–117.

[9]Brooks, T. M., Pope, D. S., and Macolini, M. A., "Airfoil Self Noise and Prediction," NASA RP-1218, 1989.

[10]Goldstein, M. E., *Aeroacoustics*, McGraw–Hill, New York, 1976.

[11]Schulten, J. B. H. M., "Vane Sweep Effects on Rotor/Stator Interaction Noise," AIAA Paper 96-1694, May 1996.

[12]Kordama, H., and Namba, M., "Unsteady Lifting Surface Theory for a Rotating Cascade of Swept Blades," American Society of Mechanical Engineers, ASME Paper 89-GT-306, New York, June 1989.

[13]Glegg, S. A. L., "Airfoil Self Noise Generated in a Cascade," AIAA Paper 96-1739, May 1996.

G. M. Faeth
Editor-in-Chief